

## Thermodynamics of NASICON ( $\text{Na}_{1+x}\text{Zr}_2\text{Si}_x\text{P}_{3-x}\text{O}_{12}$ )\*

U. WARHUS,† J. MAIER,‡ AND A. RABENAU

*Max-Planck-Institut für Festkörperforschung, Heisenbergstrasse 1,  
D-7000 Stuttgart 80, Federal Republic of Germany*

Received February 6, 1987

It is shown that Hong's NASICON solid solution range is intrinsically stable for  $T > 600$  K. With the help of electrochemical and calorimetric experiments, complete thermochemical information of  $\text{Na}_{1+x}\text{Zr}_2\text{Si}_x\text{P}_{3-x}\text{O}_{12}$  ( $0 \leq x \leq 3$ ) compositions has been elucidated, i.e., formation enthalpies, standard entropies, and molar volume (1.5–1000 K). For the purpose of a precise evaluation of the electrochemical values the specific heats of  $\text{ZrP}_2\text{O}_7$  and  $\text{Na}_2\text{ZrSi}_2\text{O}_7$  have also been determined. A thermodynamic mixture model is constructed showing that the solid solution is entropy stabilized. The energetic interaction has a destabilizing influence. The zero-point entropy and the excess entropy at higher temperatures suggest a partial ordering (Si/P) at higher temperatures. A miscibility gap, however, which is predicted for  $T \leq 600$  K by the model, could not be found due to the slow kinetics or because of a simultaneous phase transformation. The obtained values clearly show that NASICON is thermodynamically unstable with respect to a reaction with elementary sodium. The instability increases with increasing P content. © 1988 Academic Press, Inc.

### Introduction

In spite of the outstanding transport properties of the NASICON solid solution system, e.g.,  $\text{Na}^+$  conductivity of  $\text{Na}_3\text{Zr}_2\text{Si}_2\text{PO}_{12}$  amounts to  $0.2 \Omega^{-1} \text{cm}^{-1}$  at 600 K, and its high potential technological importance for the Na-S cell (1), surprisingly, no systematic investigations of the thermodynamic behavior of these compositions have been performed. In this paper we give a thorough discussion of the data obtained by thermochemical and electrochemical investigations; in particular a con-

sistent thermodynamic mixture model will be constructed. A description of the measurements, as well as a preliminary thermodynamic discussion, has been given elsewhere (2) (see also (3)).

With these data the affinities of relevant reactions with the electrode materials, which are of substantial interest for a possible application in a Na-S cell, are calculated.

Apart from this, even the intrinsic stability of Hong's classical solid solution range,  $\text{Na}_{1+x}\text{Zr}_2\text{Si}_x\text{P}_{3-x}\text{O}_{12}$  ( $0 \leq x \leq 3$ ) (4), in the following denoted by  $\text{Nas}(x)$ , has been doubted (5, 6). Although a two-dimensionally extended, but quite limited (3, 7) composition range with varying Na/Zr ratio ( $\text{Na}_{1+x+4y}\text{Zr}_{2-y}\text{Si}_x\text{P}_{3-x}\text{O}_{12}$ ) has been shown to exist (8), we restrict our attention to the linear range which can be considered as a

\* Dedicated to John B. Goodenough.

‡ To whom correspondence should be addressed.

† Present address: Bayerisches Geoinstitut, Universität Bayreuth, 8580 Bayreuth, Federal Republic of Germany.

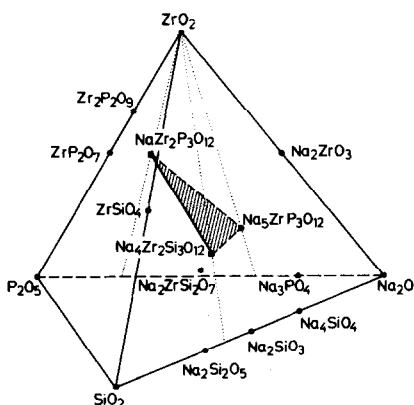


FIG. 1.  $\text{Na}_2\text{O}-\text{SiO}_2-\text{ZrO}_2-\text{P}_2\text{O}_5$  tetrahedron showing the NASICON solid solution as well as other relevant phases.

solid mixture of the two end-members  $\text{NaZr}_2\text{P}_3\text{O}_{12}$  and  $\text{Na}_4\text{Zr}_2\text{Si}_3\text{O}_{12}$ .

The NASICON composition together with other relevant phases are plotted in the  $\text{Na}_2\text{O}-\text{ZrO}_2-\text{SiO}_2-\text{P}_2\text{O}_5$  phase tetrahedron in Fig. 1.

## Experimental

The experimental part of the investigation is discussed in detail elsewhere (2, 3) and only the main features are presented here.

The synthesis of single-phase NASICON materials has been performed chiefly according to two routes:

(i) A sol-gel process for the P-rich phases,  $\text{Na}_s$  ( $0 \leq x \leq 1.8$ ), which is slightly modified with respect to Ref. (9).

(ii) A dry oxidic process for the Si-rich phases,  $\text{Na}_s$  ( $1.5 \leq x \leq 3$ ), facilitated by the formation of liquid intermediates in which the use of  $\text{ZrP}_2\text{O}_7$  as the P source and as a partial Zr source is advantageous because the reaction kinetics are much faster than with  $\text{ZrO}_2$ , preventing phosphorus from escaping the system (see also Ref. (7)).

The optimized procedures are presented as flow diagrams in Figs. 2A and 2B. The products have been characterized by weight control, density and differential

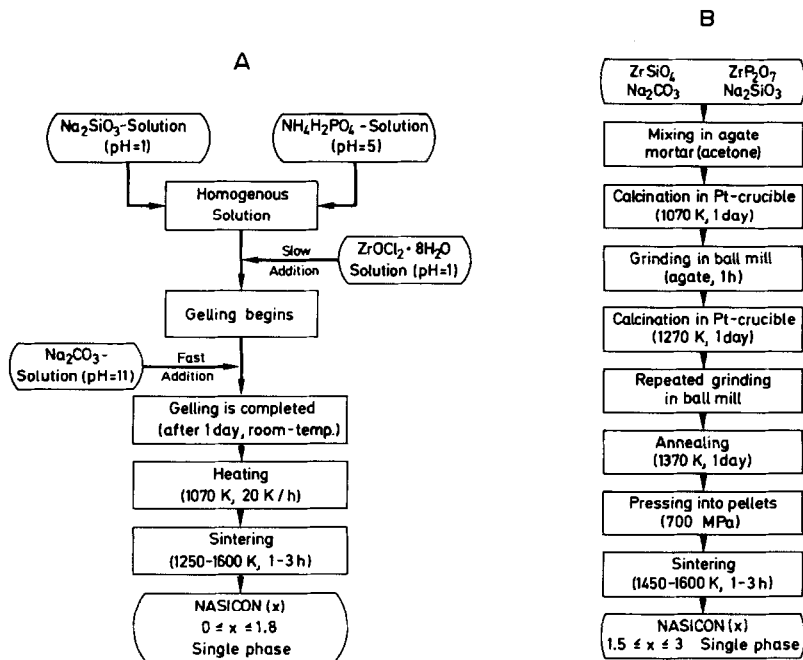


FIG. 2. Flow diagrams showing optimized preparation methods. (A) Sol-gel process for  $\text{Na}_s$  ( $0 \leq x \leq 1.8$ ). (B) Dry oxidic process for  $\text{Na}_s$  ( $1.5 \leq x \leq 3$ ).

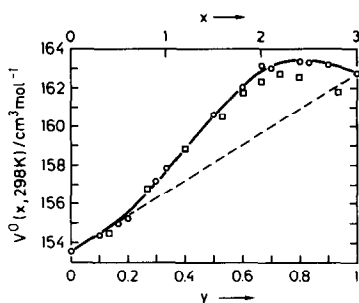


FIG. 3. Molar volume as a function of  $x$ . The square symbols refer to Ref. (4).

scanning calorimetry (DSC) measurements, chemical analysis, and optical (IR, polarization microscope) and X-ray investigations. For long-term stability tests, the ceramic specimens were annealed in tightly closed Pt capsules.

In order to obtain quantitative thermodynamical information two techniques were applied:

(i) The emf of a galvanic formation cell (2, 10) was measured as a function of temperature ( $T = 900$ – $1300$  K) under different ambient conditions.

(ii) The specific heat was determined as a function of temperature ( $1.2$ – $800$  K) by adiabatic and by differential scanning calorimetry.

## Results

Fifteen different compositions were prepared. Their molar volumes are represented in Fig. 3. The values agree with recent literature data (11–13) but deviate distinctly from Hong's original findings in the range of  $x = 2.4$ – $3$ . In regard to stoichiometry we estimate the accuracy to about  $\sim 5\%$ , which is quite adequate for our thermodynamic investigations. The difference from linearly interpolated values, i.e., the excess volume, exhibits a maximum at  $x = 2$ , where the highest ionic conductivity and the lowest activation energy are found. The influence of packing density on the bottle-

neck of the  $\text{Na}^+$  conduction path (14) is obvious. Moreover, the shape of the  $V^0$ - $x$  curve is typical for similarly complex silicate systems (15).

Long-term durability tests do not reveal demixing or decomposition. Systematic variation of the preparation conditions suggest that the following reasons are responsible for the failure of many attempts in the literature to prepare single-phase Nas( $x$ ):

(i) Insufficient reaction rates due to unfavorable selection of educts or due to an unfavorable size and distribution of the reactants.

(ii) Synthesis at too high temperatures, resulting in decomposition with  $\text{ZrO}_2$  precipitation (2, 10).

(iii) Volatilization of Na and of P compounds.

These imperfect conditions lead to heterogeneous products mostly with  $\text{ZrO}_2$  (7) or glassy compositions (2, 6) as second phases. In particular, the IR spectra compiled in Fig. 4 agree with literature findings (16) and show no evidence of condensed silicate or phosphate groups (5).

With the help of the emf cells, the enthalpies and the entropies of the following reac-

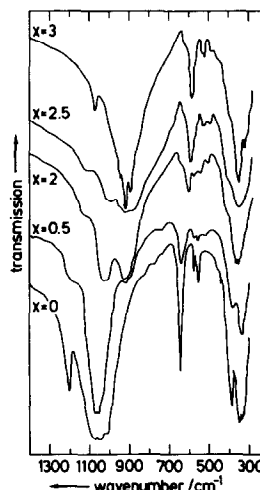


FIG. 4. Infrared spectra for different Nas( $x$ ) at 298 K.

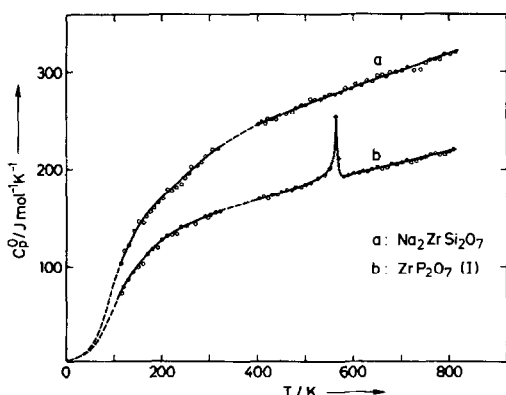
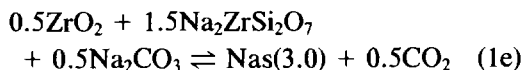
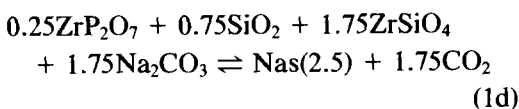
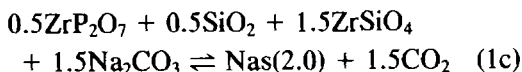
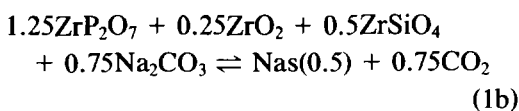
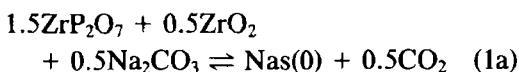


FIG. 5. Specific heats for (a)  $\text{Na}_2\text{ZrSi}_2\text{O}_7$  and (b)  $\text{ZrP}_2\text{O}_7$  as a function of temperature.

tions have been determined ( $T = 900\text{--}1300$  K) (2).



The thermodynamic data of the co-reactants that are necessary for the calculation of the desired values for  $\text{Nas}(x)$  have been taken from the literature (3, 17–20) and are compiled in Appendix I.<sup>1</sup> Only for  $\text{Na}_2\text{ZrSi}_2\text{O}_7$ , where the experimental entropy values, and for  $\text{ZrP}_2\text{O}_7$ , where both the experimental entropy and enthalpy values were

<sup>1</sup> The problem of a possible formation of a  $\text{Zr}_2\text{P}_2\text{O}_9$  phase is discussed in Ref. (3).

not available, was it necessary to measure the specific heats of these materials. This was done in the  $T$  range of 100–800 K, and the experimental curve has been extrapolated to the zero point (Debye's law). The results are presented in Fig. 5 and can be analytically given for  $T \geq 298$  K as

(a) for  $\text{Na}_2\text{ZrSi}_2\text{O}_7$

$$C_p/[\text{J mole}^{-1} \text{K}^{-1}] = 1307 - 8.88 \times 10^{-1}(T/\text{K}) + 8.00 \times 10^6 (T/\text{K})^{-2} - 1.66 \times 10^4 (T/\text{K})^{-1/2} + 4.57 \times 10^{-4} (T/\text{K})^2$$

(b) for  $\text{ZrP}_2\text{O}_7$

$$C_p/[\text{J mole}^{-1} \text{K}^{-1}] = 257.3 - 2.27 \times 10^{-2}(T/\text{K}) - 2.15 \times 10^5 (T/\text{K})^{-2} - 1.78 \times 10^3 (T/\text{K})^{-1/2} + 6.69 \times 10^{-5} (T/\text{K})^2.$$

Integration over  $\ln T$ , neglecting zero-point entropy, yields the absolute entropy, e.g., for 298 K,

(a) for  $\text{Na}_2\text{ZrSi}_2\text{O}_7$ :

$$S^0(298 \text{ K}) = (248 \pm 2) \text{ J mole}^{-1} \text{K}^{-1} \text{ (cf. estimated values 225 and 209 J mole}^{-1}\text{; Appendix II)}$$

(b) for  $\text{ZrP}_2\text{O}_7$  (I):

$$S^0(298 \text{ K}) = (189 \pm 2) \text{ J mole}^{-1} \text{K}^{-1} \text{ (cf. estimated values 166 and 196 J mole}^{-1}\text{K}^{-1}\text{; Appendix II)}$$

For the formation enthalpy of  $\text{ZrP}_2\text{O}_7$  (I) only one estimated value for  $T = 298$  K (see Appendix II) of  $-2645 \text{ kJ mole}^{-1}$  is available (21). The enthalpy and entropy of the transition from the low-temperature form (I) to the high-temperature form are small ( $\Delta H \approx 0.7 \text{ kJ mole}^{-1}$ ,  $\Delta S \approx 1.2 \text{ J mole}^{-1} \text{K}^{-1}$ ). The uncertainty of the above value represents the main error source of our thermodynamic calculations.

The  $C_p^0$  values for different NASICON compositions ( $T = 1.5\text{--}800$  K), viz.,  $\text{Nas}(0, 1, 2, 3)$ , have already been published (2). The increase of  $C_p$  with increasing  $x$  in the high-temperature range, which is shown there, reflects nicely the augmentation of the particle number per formula unit,  $N$

TABLE I  
COEFFICIENTS OF THE THERMODYNAMIC FUNCTIONS

$10^{-3}A$ (J mole <sup>-1</sup> K <sup>-1</sup> )	$B$ (J mole <sup>-1</sup> K <sup>-2</sup> )	$10^{-7}C$ (J K mole <sup>-1</sup> )	$10^{-4}D$ (J mole <sup>-1</sup> K <sup>-0.5</sup> )	$10^3E$ (J mole <sup>-1</sup> K <sup>-3</sup> )	$10^{-4}K_S$ (J mole <sup>-1</sup> K <sup>-1</sup> )
0.3882	0.1013	-0.4665	-0.0974	-0.0000	-0.2016
-4.5203	4.8522	-5.5903	7.2820	-2.2061	3.2909
0.8059	-0.6685	-1.5617	-0.2120	0.4866	-0.4328
-0.6819	1.1106	-1.9364	1.6671	-0.4300	0.5821
3.8754	-2.8147	3.5091	-5.4749	1.1809	-2.7013
$10^{-3} \Delta_f A$ (J mole <sup>-1</sup> K <sup>-1</sup> )	$\Delta_f B$ (J mole <sup>-1</sup> K <sup>-2</sup> )	$10^{-7} \Delta_f C$ (J K mole <sup>-1</sup> )	$10^{-4} \Delta_f D$ (J mole <sup>-1</sup> K <sup>-0.5</sup> )	$10^3 \Delta_f E$ (J mole <sup>-1</sup> K <sup>-3</sup> )	$10^{-6} \Delta_f K_H$ (J mole <sup>-1</sup> )
-0.0467	0.1275	-0.5604	0.1091	-0.0583	-4.9370
-4.9720	4.8797	-5.6871	7.4895	-2.2606	-6.6070
0.3042	-0.6371	-1.6672	-0.0015	0.4436	-5.9290
-1.2004	1.1433	-2.0449	1.8786	-0.4692	-6.4441
3.3402	-2.7807	3.3977	-5.2624	1.1455	-5.2369

( $\Delta N/\Delta x = 1$ ;  $\Delta C_p/\Delta x \approx 3R$ ). (The low-temperature behavior will be discussed in detail elsewhere.) This information allows us to elucidate the formation enthalpy  $\Delta_f H^0$  and the absolute standard entropy  $S^0$  for the whole  $x$ - $T$  range of interest. The relevant thermodynamic functions above room temperature can be represented as

$$C_p^0(x, T) = A(x) + B(x)T + C(x)T^{-2} + D(x)T^{-1/2} + E(x)T^2 \quad (2)$$

$$S^0(x, T) = K_s(x) + A(x) \ln T + B(x)T - \frac{1}{2}C(x)T^{-2} - 2D(x)T^{-1/2} + \frac{1}{2}E(x)T^2. \quad (3)$$

$$\Delta_f H^0(x, T) = K_H(x) + \Delta_f A(x)T + \frac{1}{2}\Delta_f B(x)T^2 - \Delta_f C(x)T^{-1} + 2\Delta_f D(x)T^{1/2} + \frac{1}{3}\Delta_f E(x)T^3. \quad (4)$$

The coefficients are listed in Table I. The data have been thoroughly reevaluated and the accuracy has been improved compared to the values given in Ref. (2) by using the new experimental  $C_p$  values of  $\text{Na}_2\text{ZrSi}_2\text{O}_7$  and of  $\text{ZrP}_2\text{O}_7$ .

The thermochemical values computed for 800 K and for 298 K (metastable region) together with estimated values are presented in Table II.

TABLE II  
THERMOCHEMICAL VALUES FOR 298 AND 800 K OF Nas(x)

	$\Delta_f H_{298}^0$ (kJ mole <sup>-1</sup> )	$\Delta_f H_{800}^0$ (kJ mole <sup>-1</sup> )	$S_{298}^0$ <sup>a</sup> (J mole <sup>-1</sup> K <sup>-1</sup> )	$S_{800}^0$ <sup>a</sup> (J mole <sup>-1</sup> K <sup>-1</sup> )	$S_{298, \text{cal}}^0$ (J mole <sup>-1</sup> K <sup>-1</sup> )	$S_{800, \text{cal}}^0$ (J mole <sup>-1</sup> K <sup>-1</sup> )
0	-4889	-5133	370	738	365	733
0.5	-5115	-5320	376	755	379	770
2.0	-5813	-5891	404	826	414	842
2.5	-6044	-6086	422	847	421	857
3.0	-6285	-6286	427	865	425	862

<sup>a</sup> Electrochemically determined.

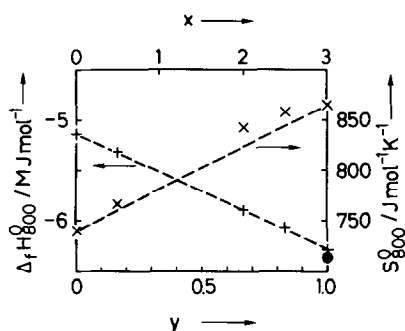


FIG. 6.  $\Delta_f H^0$  and  $S^0$  as a function of composition for 800 K (the filled circle refers to Ref. (17)).

By extrapolating the specific heats to 0 K according to Debye's  $T^3$  law and by integrating them over  $\ln T$ , the entropy—with the exception of the frozen-in configuration part—is obtained. These results are, denoted as  $S_{\text{cal}}^0$ , also given in Table II.

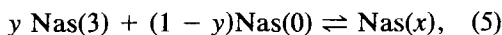
## Discussion

### Entropies and Formation Enthalpies

Figure 6 shows the formation enthalpy and the absolute entropy for  $\text{Nas}(x)$  as a function of the composition ( $T = 800$  K). The entropy shows a distinct deviation from the interpolated behavior which is similar to the behavior of the molar volume (Fig. 3). Within the resolution of the enthalpy data in Fig. 6, no deviations from a straight line can be seen. It is obvious that our enthalpy value for  $\text{Nas}(3)$  is supported, rather than the experimental literature value (27), which is also plotted in Fig. 6.

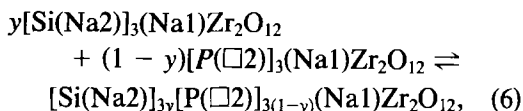
### Mixture Model: General Considerations

For a more detailed discussion of the values it is useful to consider  $\text{Nas}(x)$  as a mixture of the end-members  $\text{Nas}(0)$  and  $\text{Nas}(3)$  according to



where  $y = x/3$  is the mole fraction of the Si end-member. Since with increasing  $x$  (or  $y$ )

phosphorus is replaced by silicon and simultaneously a vacancy on a so-called (Na2) site is occupied by a further sodium (14), Eq. (5) can be written more clearly as



indicating that we have a mixture of three structure units per formula unit with the  $(\text{Na}1)\text{Zr}_2\text{O}_{12}$  unit unchanged. To a first approximation, it is assumed that the structure elements Si and (Na2), as well as P and  $(\square 2)$ , are strictly coupled such that no independent mixing of (Na2) and  $(\square 2)$  occurs, although this could be possible on structural grounds. With this assumption the entropy change of an ideal mixing process with respect to 1 mole of  $\text{Nas}(x)$  reads

$$\Delta_M S^{\text{id}} = k \ln \left\{ \frac{(\alpha N)!}{(y\alpha N)!((1-y)\alpha N)!} \right\} \approx -R\alpha \{ y \ln y + (1-y) \ln(1-y) \} \quad (7)$$

where  $\alpha$  is the number of independently mixing structure units per formula unit and  $N$  is Avogadro's number. For  $\alpha = 3$  we have

$$\Delta_M S^{\text{id}} = -R \left\{ x \ln \frac{x}{3} + (3-x) \ln \frac{3-x}{3} \right\} = -\frac{\Delta_M G^{\text{id}}}{T}. \quad (8)$$

The last identity is valid because for ideal mixtures the enthalpy of mixing vanishes ( $\Delta_M H^{\text{id}} = 0$ ).

Already the shape of  $V^0(x)$  and the misfit,  $V^0(3) - V^0(0)$ , in Fig. 3, have demonstrated that ideal behavior cannot be expected. For constructing a mixture model it is convenient to consider just the excess of the different functions of state ( $Z$ ) over their values in the case of ideal mixing ( $Z^{\text{ex}} = \Delta_M Z^0 - \Delta_M Z^{\text{id}}$ ). In this way  $H^{\text{ex}}$  ( $= \Delta_M H^0$ ),  $S^{\text{ex}}$ , and  $V^{\text{ex}}$  are defined. Since the contribution of the educts ( $Z(0)$  and  $Z(3)$ ) cancels in

the difference,  $Z^{\text{ex}}$  refers to  $\text{Nas}(x)$  directly and for this reason the operator  $\Delta_{\text{M}}$  has been dropped.

Analyzing the enthalpy of mixing for a real mixture, it can be shown (22) that it is useful to write

$$G^{\text{ex}}(y, T) = \Omega_G(y, T)y(1 - y). \quad (9)$$

The parameter  $\Omega_G$  vanishes in the case of an ideal mixture, it is constant with respect to  $y$  for a so-called regular mixture ( $\Omega_G(y, T) = W_G(T)$ ), and linear for a simple subregular mixture ( $\Omega_G(y, T) = W'_G(T)y + W''_G(T)(1 - y)$ ).

Asymmetric mixtures of higher orders have to be described by using higher order polynomials.  $\Omega_G$  can be broken up into

$$\Omega_G(y, T) = \Omega_H(y, T) - T\Omega_S(y, T), \quad (10)$$

resulting in relations for  $H^{\text{ex}}$  and  $S^{\text{ex}}$  which are analogous to Eq. (9). As long as  $C_p^{\text{ex}} = \Delta_{\text{M}}C_p^0 - \delta\Delta_{\text{M}}H^{\text{id}}/\delta T = \Delta_{\text{M}}C_p^0$  can be neglected,  $\Omega_H$  and  $\Omega_S$  are independent of the temperature. The free enthalpy of  $\text{Nas}(x)$  for the whole  $x$ - $T$  range, where the mixture model is fulfilled, is given by

$$\begin{aligned} \Delta_{\text{M}}G(x, T) = & \left[ \Omega_H(x, T) \frac{x(3-x)}{9} \right] \\ & + \left[ \alpha RT \left( \frac{x}{3} \ln \frac{x}{3} + \frac{3-x}{3} \ln \frac{3-x}{3} \right) \right. \\ & \left. - RT\Omega_S(x, T) \frac{x(3-x)}{9} \right]. \quad (11) \end{aligned}$$

The first bracketed term describes the energetic interaction, which may or may not be favorable for the formation of a solution, and the second one the entropy change of the mixing process. The latter part of the entropy term results chiefly from vibronic changes and may be positive or negative, whereas the first part describes the configurational entropy which must always favor a solid solution. As it is well-known, the  $\Delta_{\text{M}}G$  vs  $x$  curve is of a double-minimum shape at those temperatures where a decomposition within the mixture range, i.e., a miscibility

gap, is demanded by the thermodynamic properties. The equilibrium compositions of the coexisting phases ( $\text{Nas}(x_A)$ ,  $\text{Nas}(x_B)$ ) can be obtained by constructing the double tangent (22). The two inflection points between  $x_A$  and  $x_B$  limit the region of spinodal decomposition. By increasing the temperature, the mixture is more and more favored and the  $\Delta_{\text{M}}G(x, T)$  curve takes a one-minimum form, indicating complete miscibility. At the critical points, the inflection points coincide meaning that

$$\frac{d^2\Delta_{\text{M}}G(x, T_{\text{cr}})}{dx^2} \Big|_{x=x_{\text{cr}}} = \frac{d^3\Delta_{\text{M}}G(x, T_{\text{cr}})}{dx^3} \Big|_{x=x_{\text{cr}}} = 0. \quad (12)$$

From Eq. (12) the critical values  $T_{\text{cr}}$ ,  $x_{\text{cr}}$  can be obtained. Eq. (11) allows us to elucidate the chemical potential, the activity, and the activity coefficient of the end-members in the solid solution  $\text{Nas}(x)$ . If we consider a third of the formula unit (index  $\frac{1}{3}$ ), we have in the case of an ideal mixture ( $\Omega_H = \Omega_S = 0$ ) for the chemical potential of  $\text{Nas}(\frac{1}{3})$ :  $\mu_{1/3} = \mu_{1/3}^0 + RT \ln y$ . In the case of a real mixture the activity of  $\text{Na}_{4/3}\text{Zr}_{2/3}\text{SiO}_4$  ( $= \frac{1}{3} \text{Nas}(3)$ ),  $a_{1/3} = f_{1/3}y$ , has to be introduced instead of  $y$ , with the activity coefficient being given by

$$\begin{aligned} 3RT \ln f_{1/3} = & (2W'_G - W''_G)(1 - y)^2 \\ & + 2(W''_G - W'_G)(1 - y)^3. \quad (13) \end{aligned}$$

#### Mixture Model: Comparison with the Results

In Fig. 7 the entropy and the enthalpy are divided by  $y(1 - y)$  and plotted against the composition for 800 K. The linear relationship means that the mixture can be satisfactorily described by a simple subregular mixture model. The  $W$  parameters for 800 K are  $W'_{H800} = 59 \text{ kJ mole}^{-1}$ ,  $W''_{H800} = 33 \text{ kJ mole}^{-1}$ ;  $W'_{S800} = 40 \text{ J mole}^{-1} \text{ K}^{-1}$ ,  $W''_{S800} = 33 \text{ J mole}^{-1} \text{ K}^{-1}$  if  $\alpha = 3$  is assumed.<sup>2</sup>

Obviously  $C_p^{\text{ex}}$  is small and the tempera-

<sup>2</sup> The  $W_H$  parameters are distinctly greater than the values that are expected for a pure silicate system (3).

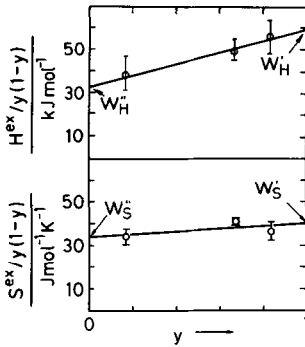


FIG. 7.  $\Omega_H$  (top) and  $\Omega_S$  (bottom) as a function of composition.

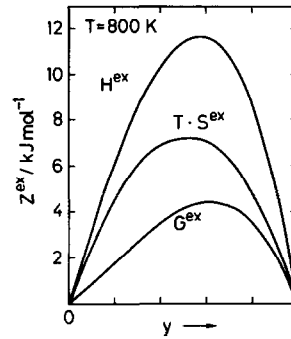


FIG. 9. Representation of the excess functions  $G^{ex}(x)$ ,  $H^{ex}(x)$ ,  $S^{ex}(x)$ , for 800 K.

ture variation of the  $W$  parameters can to a first approximation be neglected (Fig. 8).

This especially holds for  $W'_H$  and  $W''_H$ , whereas the change of  $W'_S$  and  $W''_S$  is perceptible. Interestingly the difference between the  $W_S$  parameters between 800 and 298 K can be nearly completely removed, if for 298 K,  $\alpha = 1$  is assumed. This is a first indication of an ordering of ions in tetrahedral positions (Si,P), which has also been reported in the literature (23, 24). Astonishingly the finding  $\alpha = 1$  is close to Wuensch's X-ray results (23).

Figure 9 represents the excess enthalpy and the excess entropy for 800 K which are, because of  $C_p^{ex} \approx 0$ , roughly representative for the whole  $T$  range.  $\Delta_M H^0 = H^{ex}$  is positive over the whole composition range meaning that the energetic interaction destabilizes the mixture. Since  $\Delta_M G^0$  is negative (i.e., the mixture is stable against a decomposition into the end-members), as it is revealed by Fig. 10, the mixture is completely entropy stabilized. Even the excess entropy is positive (Fig. 9), as is well-known for comparable silicate systems,

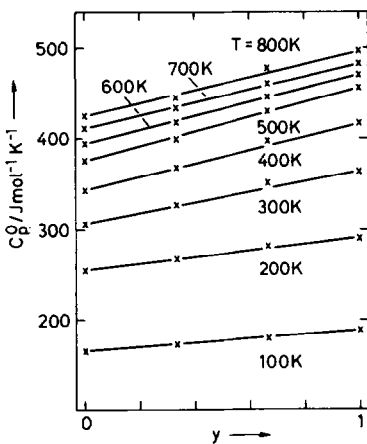


FIG. 8.  $C_p^0$  as a function of  $x$  for different temperatures (corrected with respect to the phase transformations).

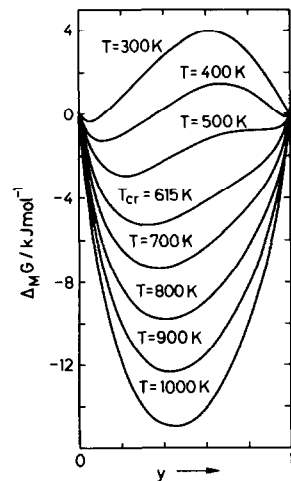


FIG. 10. The free enthalpy of mixing as a function of composition.



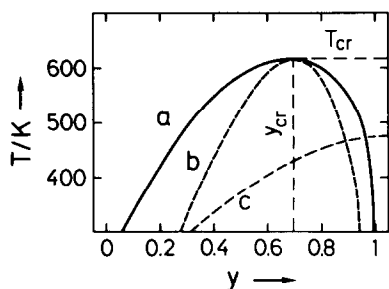


FIG. 11. Calculated miscibility gap (a), calculated spinode (b), and experimentally determined phase transformation line (c) (see text).

e.g., for garnets such as  $\text{Mg}_{3x}\text{Ca}_{3-3x}\text{Al}_2\text{Si}_3\text{O}_{12}$  or pyroxenes such as  $\text{Ca}_{2x}\text{Mg}_{2-2x}\text{Si}_2\text{O}_6$  (25). Figure 10 also indicates the formation of a miscibility gap for  $T \leq 600$  K with the critical point of demixing ( $T_{cr}; x_{cr}$ )  $\approx (600 \text{ K}; 2)$  as represented in Fig. 11. Such a miscibility gap has not been found experimentally, owing to the slow kinetics of reorganization. Nevertheless, the similar values of  $S_{cal}^0$  and  $S^0$  in Table II suggest a low zero-point entropy, which is distinctly lower than the configurational part formulated in Eq. (8) and even more so if independent mixing of (Na2) and ( $\square$ 2) is assumed. Consequently, in agreement with the above considerations, a partial ordering is probable. Unfortunately, our electrochemical values are not precise enough for detailed conclusions. If we consider slightly lower  $\alpha$  values even for higher temperatures, the maximum for  $S^{ex}$  (Fig. 9) shifts toward  $x = 2$  which would be expected for a pure vibronic contribution.

At a first glance the kinetic intrinsic stability of  $\text{Nas}(x)$  seems to contradict the assumption of a partial ordering. But first of all the exact temperature of critical mixing ( $\Delta T \approx 100$  K) depends sensitively on our experimental uncertainties concerning the  $W_H$  parameters and in particular concerning  $\Delta_f H^0(\text{ZrP}_2\text{O}_7)$ ; second, the mechanisms of demixing and of ordering should be different, and, third, the system seems to evade

the demixing process by a phase transformation (3, 26, 27) (see curves a and c in Fig. 11).

Although we are not concerned with the pressure dependence, we should add that the knowledge of  $V^{ex}$  allows us to give the excess energy  $U^{ex}$  as well as the pressure dependence of  $G^{ex}$  according to

$$U^{ex} = H^{ex} - pV^{ex}, \quad (15)$$

where

$$V^{ex} = (\delta G^{ex}/\delta p)_{T,y}. \quad (16)$$

Tentatively representing  $V^{ex}$  as  $yW_V^{\prime} + (1-y)W_V^{\prime\prime}$ , we find from Fig. 12 that  $W_V^{\prime} = 28 \text{ cm}^3 \text{ mole}^{-1}$  and  $W_V^{\prime\prime} = -5.5 \text{ cm}^3 \text{ mole}^{-1}$  (for 298 K).

All the thermodynamic information that is of interest here ( $x, T$  dependence) can be roughly summarized by

$$G^{ex}(x, T) = (11x - 0.78x^2 - 0.96x^3) \text{ kJ mole}^{-1} - T(11x - 2.9x^2 - 0.26x^3) \text{ J mole}^{-1} \text{ K}. \quad (17)$$

With these model parameters the activities of the end-members in the mixture have been calculated according to Eq. (13). The results for the activity of the Si end-member are shown in Fig. 13 where  $\alpha = 3$  is assumed for the entire range. The disappearance of the nonideality with increasing temperature is obvious.

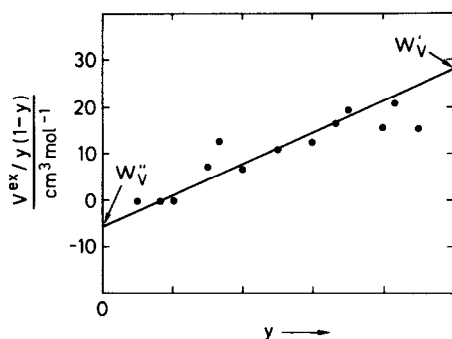


FIG. 12.  $V^{ex}/(y(1-y))$  as a function of composition.

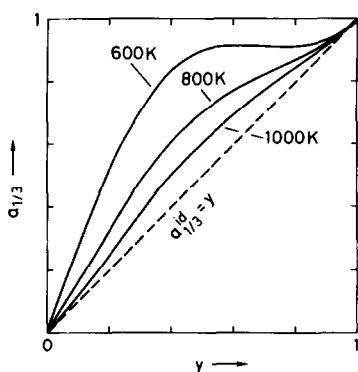
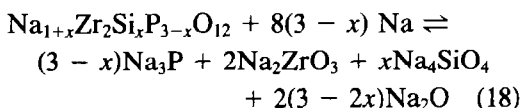


FIG. 13. The activity of  $\frac{1}{3}\text{Nas}(3)$  in the NASICON solid solution for a frozen-in Si-P disorder ( $\alpha = 3$ ).

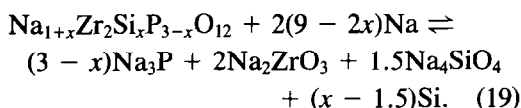
### Stability against Sodium

An important application of the above results is the calculation of the affinities of possible reactions of  $\text{Nas}(x)$  with elementary sodium. The reactions with the highest affinities are

(a) for  $0 \leq x \leq 1.5$



(b) for  $1.5 \leq x \leq 3.0$



Since the excess values are negligible for the calculation of the free enthalpy of reaction, the  $\Delta_{\text{deg}}G(x)$  curve (deg: degradation reaction) consists of two linear branches. Also the problem of ordering is not important here so that  $\alpha = 3$  is assumed for the calculations. The relevant data, refined compared to Ref. (2), are collected in Table III. The values for the reaction partners can be found in Appendix I. The main error sources are the formation enthalpy of  $\text{Na}_4\text{SiO}_4$  (see Appendix I) as well as  $S^0$  and  $C_p^0$  of  $\text{Na}_3\text{P}$  which had to be estimated (Appendix II). The general conclusions, how-

ever, are not affected by these uncertainties. According to Table III,  $\text{Nas}(x)$  is thermodynamically unstable with respect to a reaction with sodium for all values of  $x$ . The instability is even increased by about  $1\text{--}100\text{ kJ mol}^{-1}$  if a further reaction leading to  $\text{NaSi}$  instead of  $\text{Si}$  is assumed. Since quantitative data are lacking for  $\text{NaSi}$ , this reaction has not been included in Table III. This instability of  $\text{Nas}(x)$  decreases with decreasing P content. The Si end-member is close to the border of stability. A reduction to Si as demanded by thermodynamics for the Si-rich compositions could not be found experimentally (28), probably because of the great kinetic inertia of the  $\text{SiO}_4$  tetrahedra. Thus, the experimental result that  $\text{Nas}(3)$ , and not Si, is formed during the reaction of the P-containing compositions can be understood. For the same reason,  $\text{Nas}(3)$  itself is not corroded by Na, if we disregard the observed formation of color centers (27). Analogous behavior is found with respect to sulfur. Though thermodynamically unstable, no reaction is observed experimentally for  $\text{Nas}(3)$  (3, 28). Unfortunately, the bulk conductivity of this compound is poor.

As shown by our results, successful application of NASICON as an electrolyte in the Na-S cell must be doubted.

It can hardly be assumed that the reaction kinetics for the very conductive mate-

TABLE III  
THERMODYNAMIC STABILITY OF  $\text{Nas}(x)$   
AGAINST Na

$x$	$\Delta_{\text{deg}}G_{298}^0$ (kJ mole $^{-1}$ )	$\Delta_{\text{deg}}G_{600}^0$ (kJ mole $^{-1}$ )
0.0	-1081	-900
0.5	-1048	-896
1.0	-1016	-893
1.5	-983	-889
2.0	-709	-632
2.5	-435	-375
3.0	-161	-118

rials can be sufficiently depressed by optimizing the microstructure.

An application in a room-temperature battery, however, seems to be possible (29). Activities to improve the conductivity properties have been reported (27).

At present we do not see a chance for NASICON to replace the  $\beta$ -aluminas as solid electrolytes in high-performance devices.

## Appendix I

### Auxiliary Thermochemical Data

Auxiliary thermochemical data used in the text are compiled in Table AI ( $C_p = A + BT + CT^{-2} + DT^{-1/2} + ET^2$ ) and Table AII ( $\Delta_f G^0$ ;  $\Delta_f H^0$ ,  $S^0$ ).

## Appendix II

### Estimation Methods (3, 31–37)

Table AIII gives the estimation results.

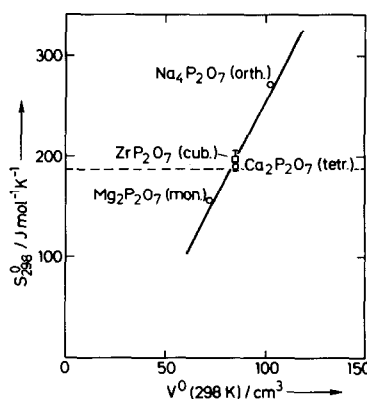


FIG. A1. Estimation of  $S^0_{298}$  for  $ZrP_2O_7$ . The experimentally determined value is indicated (dashed line).

Method a: Use of a more or less empirical relationship (e.g.,  $S^0 = S^0(V^0)$ ; see Figs. A1, A2) or use of increments (e.g.,  $\Delta_f H^0$ ) for a given class of compounds or structures.

TABLE AI  
SPECIFIC HEATS<sup>a</sup> OF RELEVANT COMPOUNDS

Phase	$a$ (J mole <sup>-1</sup> K <sup>-1</sup> )	$b$ (J mole <sup>-1</sup> K <sup>-2</sup> )	$c$ (J K mole <sup>-1</sup> )	$d$ (J mole <sup>-1</sup> K <sup>-0.5</sup> )	$e$ (J mole <sup>-1</sup> K <sup>-3</sup> )	Range of validity (K)	Phase transition <sup>b</sup>	Ref.
Na(s)	14.790	4.4229	0	0	0	298–371	Tm	20
Na(l)	37.482	-1.9183	0	0	1.0644	371–1175	Ts	18
Si	31.778	0.053878	-1.4654	-1.7864	0	298–1685	Tm	18
Zr	0	2.2629	-7.2106	4.6723	-36.247	298–1136	Tp	18
P(s), red	35.859	-1.6031	-2.0482	-1.5866	1.8309	298–704	Tsub	18
P(g)	30.350	-63.500	1.1167	-2.3929	18.664	704–1800		18
O <sub>2</sub>	48.318	-0.069132	4.9923	-4.2066	0	298–1800		18
Na <sub>2</sub> O	113.97	74.857	0	-8.1335	0	298–1000	Tm	18
SiO <sub>2</sub> ( $\alpha$ )	44.603	3.7754	-10.018	0	0	298–844	Tp	18
SiO <sub>2</sub> ( $\beta$ )	58.928	1.0031	0	0	0	844–1800	Tm	18
ZrO <sub>2</sub>	90.70	0	-8.1334	-4.3877	0	298–1478	Tp	18
ZrSiO <sub>4</sub>	236.95	-1.7879	-1.4960	-22.678	0	298–1600		18
Na <sub>4</sub> SiO <sub>4</sub>	162.59	7.4224	0	0	0	298–1393	Tp	20
Na <sub>2</sub> ZrSi <sub>2</sub> O <sub>7</sub>	1306.7	-88.836	79.9809	-166.388	45.71	298–810		3
Na <sub>2</sub> ZrO <sub>3</sub>	412.7	-14.83	12.54	-44.98	4.115	298–1170	Tp = 1125 K	10
ZrP <sub>2</sub> O <sub>7</sub>	257.29	-2.266	-2.146	-17.837	6.693	298–810	Tp = 570 K	3
Na <sub>2</sub> CO <sub>3</sub>	11.016	24.4036	24.493	0	0	298–723	Tp	30
Na <sub>3</sub> P	110.38	-2.15	2.05	-1.59	5.57	298–(544)	Tm(Bi)	3
CaO	52.422	36.734	0	-0.5099	-7.5068	298–1800		18
CaCO <sub>3</sub>	99.715	2.6920	0	0	-21.576	298–1200		18
CO <sub>2</sub>	87.820	-26.442	+7.0641	-9.9886	0	298–1800		18

<sup>a</sup>  $C_p = a + 10^{-2}bT + 10^5cT^{-2} + 10^2dT^{-1/2} + 10^{-5}eT^2$ .

<sup>b</sup> Tm, melting temperature; Tp, transition temperature; Tsub, sublimation temperature.

TABLE AII  
 THERMODYNAMIC VALUES OF RELEVANT COMPOUNDS

Phase	$\Delta_f H_{298}^0$ (kJ mole <sup>-1</sup> )	$\Delta_f G_{298}^0$ (kJ mole <sup>-1</sup> )	$S_{298}^0$ (J mole <sup>-1</sup> K <sup>-1</sup> )	$C_{p,298}^0$ (J mole <sup>-1</sup> K <sup>-1</sup> )	$V_{298}^0$ (cm <sup>3</sup> mole <sup>-1</sup> )	Ref.
Na	0	0	51.30	28.23	23.812	18
Si	0	0	18.81	19.94	12.056	18
Zr	0	0	38.99	25.37	14.016	18
P	0	0	22.85	21.21	17.2	18
S	0	0	31.8	22.72	15.511	18
O <sub>2</sub>	0	0	205.15	29.37	24789.2	18
Na <sub>2</sub> O	-414.82	-376.09	75.27	69.10	25.88	18
SiO <sub>2</sub>	-910.70	-856.29	41.46	44.54	22.688	18
ZrO <sub>2</sub>	-1100.56	-1042.79	50.38	56.14	21.15	18
P <sub>2</sub> O <sub>5</sub>	-1470.00	-1337.90	115.50	105.86	59.4	18
ZrSiO <sub>4</sub>	-2033.4	-1918.89	84.03	98.60	39.26	18
Na <sub>4</sub> SiO <sub>4</sub>	-2082.8 <sup>a</sup>	-1975.3 <sup>a,b</sup>	195.81	184.2	69.07	20
Na <sub>2</sub> ZrSi <sub>2</sub> O <sub>7</sub>	-3606.2	-3412.4	247.6	208.8	89.81	19, 3
Na <sub>2</sub> ZrO <sub>3</sub>	-1667.8	-1570.8	126.8	125.9	45.41	10
ZrP <sub>2</sub> O <sub>7</sub>	-2645.3 <sup>a</sup>	-2469.5 <sup>a</sup>	188.8	150.7	84.38	21, 3
Na <sub>3</sub> P	-92.5	-85.4 <sup>a</sup>	155.5 <sup>a</sup>	124.6	56.89	19, 3
Na <sub>2</sub> CO <sub>3</sub>	-1130.77	-1048.1	138.78	111.33	41.62	30
CaO	-635.09	-603.48	38.21	42.12	16.764	18
CaCO <sub>3</sub>	-1207.37	-1128.84	91.71	83.47	36.934	18
CO <sub>2</sub>	-393.51	-394.38	213.79	37.13	24789.2	18

<sup>a</sup> Estimated value.<sup>b</sup> Value of Ref. (20) contradicts the phase relations (3).

Method b: Consideration of an appropriate reaction whose formation quantity can be neglected to a sufficiently good approximation. The approximation is better the lower the involved change. A more sophisticated method consists of performing this

procedure for different types of reactions and extrapolating the results to the value corresponding to a "zero-reaction" (b\*) (31) (see Fig. A3).

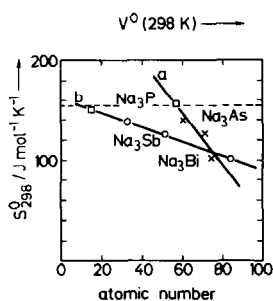

 FIG. A2. Estimation of  $S_{298}^0$  for  $\text{Na}_3\text{P}$  (a,  $V^0$ ; b, atomic number). The mean value is indicated (dashed line).

 TABLE AIII  
 RESULTS OF ESTIMATION METHODS (3)

Phase	$\Delta_f G_{298}^0$ (kJ mole <sup>-1</sup> )	$S_{298}^0$ (J mole <sup>-1</sup> K <sup>-1</sup> )	Method
NaZr <sub>2</sub> P <sub>3</sub> O <sub>12</sub>	-4577.3	376.4	b*, a
	-4376.4	320, 346.6	b, a, b
Na <sub>4</sub> Zr <sub>2</sub> Si <sub>3</sub> O <sub>12</sub>	-5928.7	415, 374.5, 372.4	b*, a, a, a
	-6009.6	429.5	b, b
	-5932.7		b
Na <sub>2</sub> ZrSi <sub>2</sub> O <sub>7</sub>	-3401.6	209.4, 203.2, 207.1	b*, a, a, a
	-3394.0	225.4	b, b
	-3355.6		a
ZrP <sub>2</sub> O <sub>7</sub>	-2469.5	196, 165.9	a, a, b
	-2507.7	190.5	b, a
Na <sub>4</sub> SiO <sub>4</sub>	-1975.3	191.8	a, a
	-1947.8		b
	-2094.9	193.9	b, b
Na <sub>3</sub> P	-85.4	155.5, 176.8	b, b, b

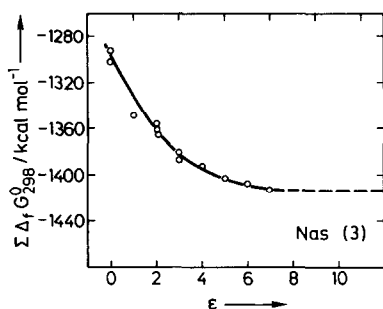


FIG. A3. Estimation of  $\Delta_r G^0$  for Nas(3). (The definition of the complexity parameter  $\epsilon$  is somewhat arbitrary (3).)

## References

1. J. B. GOODENOUGH, H. Y.-P. HONG, AND J. A. KAFALAS, *Mater. Res. Bull.* **11**, 203 (1976).
2. J. MAIER, U. WARHUS, AND E. GMELIN, *Solid State Ionics* **18/19**, 969 (1986).
3. U. WARHUS, dissertation, Universität Stuttgart (1986).
4. H. Y.-P. HONG, *Mater. Res. Bull.* **11**, 173 (1976).
5. A. CLEARFIELD, M. A. SUBRAMANIAN, W. WANG, AND P. JERUS, *Solid State Ionics* **9/10**, 895 (1983).
6. U. VON ALPEN, in "Dechema monographies 92" (W. Vielstich, Ed.), p. 135, Verlag Chemie, Weinheim (1982).
7. A. CLEARFIELD, R. GUERRA, A. OSKARRSON, M. A. SUBRAMANIAN, AND W. WANG, *Mater. Res. Bull.* **18**, 1561 (1983); A. CLEARFIELD, M. A. SUBRAMANIAN, P. R. RUDOLF, AND A. MOINI, *Solid State Ionics* **18/19**, 13 (1986).
8. H. KOHLER, H. SCHULZ, AND O. MELNIKOV, *Mater. Res. Bull.* **18**, 1143 (1983).
9. J. ALAMO, AND R. ROY, *J. Amer. Ceram. Soc.* **67**, C80 (1984).
10. J. MAIER AND U. WARHUS, *J. Chem. Thermodyn.* **18**, 309 (1986).
11. A. KRAJEWSKI, R. VALMORI, AND A. FIEGNA, *Crystallogr. Res. Technol.* **19**, 893 (1984).
12. J. ENGELL, S. MORTENSEN, AND L. MOLLER, *Solid State Ionics* **9/10**, 877 (1983).
13. L. J. SCHOILER, B. J. WUENSCH, AND E. PRINCE, private communication.
14. H. KOHLER AND H. SCHULZ, *Mater. Res. Bull.* **20**, 1461 (1985).
15. R. C. NEWTON AND B. J. WOOD, *Amer. Mineral.* **65**, 733 (1980).
16. M. BARJ, H. PERTHUIS, AND PH. COLOMBAN, *Solid State Ionics* **9/10**, 845 (1983).
17. E. V. SHIBANOV AND V. G. CHUKHLANTSEV, *Russ. J. Phys. Chem.* **48**, 133 (1974).
18. R. A. ROBIE, B. S. HEMINGWAY, AND J. R. FISHER, "Geological Survey Bulletin 1452," USGS, Washington DC (1979).
19. D. D. WAGMAN, W. H. EVANS, V. B. PARKER, R. H. SCHUMANN, I. HALOW, S. M. BAILEY, AND K. L. NUTALL, "The NBS Tables of Chemical Thermodynamic Properties," supplement to Vol. 11 of *J. Phys. Chem. Ref. Data* (1982).
20. I. BARIN, O. KNACKE, AND O. KUBASCHEKSKI, "Thermochemical Properties of Inorganic Substances," Springer-Verlag, Berlin (1973), supplement (1977).
21. N. M. FILIPPOVA AND D. I. CHEMODANOV, *Russ. J. Phys. Chem.* **49**, 158 (1975).
22. J. B. THOMSON JR., in "Research in Geochemistry" (P. H. Abelson, Ed.), p. 340, Vol. 2, New York (1969); E. A. Guggenheim, "Thermodynamics," North-Holland, Amsterdam (1986).
23. B. J. WUENSCH, L. J. SCHOILER, AND E. PRINCE, *Amer. Crystallogr. Assoc. Program Abstracts* **11**, 34 (1983).
24. P. K. DAVIES, F. GARZON, T. FEST, AND C. M. KATZAN, *Solid State Ionics* **18/19**, 1120 (1986).
25. T. GASPARIK, *Amer. Mineral.* **69**, 1025 (1984).
26. H. KOHLER AND H. SCHULZ, *Mater. Res. Bull.* **21**, 23 (1986).
27. K. D. KREUER, H. SCHULZ, AND U. WARHUS, *Mater. Res. Bull.* **21**, 149 (1986).
28. K. D. KREUER AND U. WARHUS, *Mater. Res. Bull.* **21**, 357 (1986).
29. W. DENNSTEDT, private communication.
30. D. R. STULL AND H. PROPHET, "Janaf Thermochemical Tables," 2nd ed., Vol. 37, Natl. Standard Ref. Data Ser., U.S. Natl. Bur. Standards (1971).
31. C. H. CHEN, *Amer. J. Sci.* **275**, 801 (1975).
32. S. K. SAXENA, *Science* **193**, 1241 (1972).
33. J. O. NRIAGU, *Amer. Mineral.* **60**, 834 (1975).
34. R. POWELL, "Equilibrium Thermodynamics in Petrology: An Introduction," Harper & Row, London (1978).
35. S. CANTOR, *Science* **198**, 206 (1977).
36. Y. TARDY AND R. M. GARRELS, *Geochim. Cosmochim. Acta* **41**, 87 (1977).
37. E. V. SHIBANOV AND V. G. CHUKHLANTSEV, *Russ. J. Phys. Chem.* **44**, 872 (1970).